Frontiers in Bioscience Landmark

Front. Biosci. (Landmark Ed) **2022**; 27(2): 058
http://doi.org/10.31083/j.fbl2702058

Original Research

Role of CK1ε-regulated PERIOD2 in STZ-induced diabetic myocardial injury

Qin Huang[1,†], Meng Jiang[1,†], Zhong-Yuan Xia[1,*], Shaoqing Lei[1], Bo Zhao[1], Zhen Qiu[1]

[1]Department of Anesthesiology, Renmin Hospital of Wuhan University, 430060 Wuhan, Hubei, China
*Correspondence: xiazhongyuan2005@aliyun.com (Zhong-Yuan Xia)
[†]These authors contributed equally.

Academic Editor: Kebin Hu
Submitted: 3 November 2021 Revised: 6 January 2022 Accepted: 17 January 2022 Published: 12 February 2022

Abstract

Background: Circadian rhythms are fundamental to regulating metabolic processes and cardiovascular functions. Phosphorylated PERIOD2 (PER2) is a key factor in determining the period of the mammalian circadian clock. Moreover, casein kinase 1ε (CK1ε) primes the PER2 phosphoswitch and its stability. While diabetes contributes to the disorder of the circadian system, changes in PER2 forms and their regulatory mechanisms during diabetes remain unclear. In this study, we examined the impact of diabetes on PER2 and CK1ε signaling in the heart to determine the potential mechanism between them. **Methods**: A Type-1 diabetic rat model was established by intraperitoneally injecting rats with streptozotocin. General characteristics, cardiac function, histology, serum biochemistry, apoptosis index and circadian rhythm were analyzed in controls and diabetic rats treated with or without PF-670462 (a CK1ε inhibitor). A high-glucose model was created with H9c2 cells and treated with PF-670462 and PER2 siRNA. Cell viability, LDH release, dead/live rate and histology were determined to assess cellular injuries. RT-PCR and Western blot were used to evaluate the expression of PER2, CK1ε, phosphorylated PER2, and immunofluorescence (IF) was employed to determine PER2's location. **Results**: STZ-induced diabetes prolonged PER's period and upregulated the expression of CK1ε and phosphorylated PER2 compared to the controls. Inhibiting CK1ε and PER2 with PF-670462 downregulated the phosphorylation at Ser662 and the nuclear entry of PER2 in high glucose conditions. In addition, pharmacologically or genetically suppressing PER2 mitigated high-glucose-instigated myocardial injury. **Conclusions**: Diabetes compromised PER2 in association with activated CK1ε signaling. Targeting CK1ε-regulated PER2 alleviates myocardial injuries in the presence of high glucose.

Keywords: PER2; CK1ε; phosphorylated PER2; PF-670462; diabetic myocardial injury

1. Introduction

Diabetes mellitus (DM) is a lifelong metabolic disease and its prevalence continues to increase [1,2]. DM affects myocardial morphology, metabolism, gene expression, physiological function, and much more. Diabetes-associated myocardial structural and functional changes are known as diabetic cardiomyopathy [3]. Cardiovascular complications caused by diabetic myocardial injuries are among the major causes of mortality and morbidity in diabetic patients. However, diabetes' exact pathogenesis is complicated, and there is no effective treatment method for the condition yet. Therefore, actively exploring its potential mechanism could provide a useful protective measure to reduce the incidence of diabetes-related complications.

In mammals, rhythms are orchestrated by a master time-keeping mechanism housed within the suprachiasmatic nuclei (SCN) of the hypothalamus, and peripheral organs, such as the heart, have their individual self-endogenous clocks as well. Myocardial contraction, relaxation, and effective blood pumping exhibit rhythmic fluctuations [4–6]. Increasing evidence suggests that diabetes inter-relates with disrupted circadian clock rhythms [7–10]. The circadian clock consists of multiple core proteins, including BMAL1, ClOCk, PERIOD (PER1-3) and CRYTOCHROME (CRY1-2), that interact to influence each other's transcription and function. Of these proteins, PER2 is enormous, with a well-defined N-terminal region containing PER-ARNT-SIM (PAS) domains and two unique competing phosphorylation sites [11–13]. These motifs and domains are responsible for multiple homodimeric and heterodimeric protein interactions, as well as PER's stability, cellular localization, and inhibitory activity toward CLOCK:BMAL [14–16]. Most of all, PER2 plays a significant role in the integration of signals and helps to robustly compensate for profound changes that would disrupt the circadian clock. Additionally, PER2 in the heart has a notable impact on its gene expression and overall tissue function [7,17,18]. Studies have shown that diabetes causes PER2 to exhibit massive phase shifts in mRNA levels and severely aggravated myocardial functional disorders [19,20]. It has also been demonstrated that pharmacologically targeting PER2 improves glucose homeostasis in obesity [8]. These findings collectively indicate that myocardial pathological processes during diabetes are closely associated with the clock gene PER2. However, changes in the PERIOD2 (PER2) protein forms and their exact mechanisms in diabetic myocardial injuries remain unclear.

Casein kinase 1 (CK1), a member of the superfamily of serine/threonine-specific kinases, participates in modulating various cellular activities, such as circadian rhythm and glycolipid metabolism [21–23]. CK1ε (an isoform of CK1) efficiently primes PER2 for downstream phosphorylation and determines its period and degradation rates via phosphorylation at its specific site [10,24–26]. A single amino acid modification in CK1ε (CK1ε^{tau}, R178C) disrupts PER2's operating mode [27,28]. These reports imply that CK1ε plays a conspicuous regulatory role in stabilizing the PER2 protein. Currently, CK1ε inhibitors are being examined for possible use to pharmacologically target PER2 to regulate circadian rhythms [29–31]. However, research focusing on the role of CK1ε signaling in modulating PER2 and myocardial injuries during diabetes is rare.

To explore the adaptive connection between diabetes and PER2, we have highlighted the exact impact of diabetes on PER2 and CK1ε signaling. Also, we have hypothesized and investigated whether targeting CK1ε-regulated PER2 could mitigate high-glucose-induced myocardial injuries, hoping to provide a new strategy for protection against and the treatment of diabetes.

2. Materials and methods

2.1 Animals

Male Sprague-Dawley rats (8-weeks old, weighing 180~220 g) were obtained from Beijing Vital River Laboratory Animal Technology Co, Ltd and maintained in an SPF environment at an ambient temperature of 20–22 °C, with food and water supplied ad libitum.

2.2 Drugs and chemicals

PF-670462 was purchased from Topscience, and its potency (IC50 = 7.7 $\pm$ 2.2 nM) and selective inhibition of CK1ε were confirmed first in isolated enzyme preparations before subsequent dissolution in dimethyl sulfoxide (DMSO) (used in *in vitro* experiments) and high-pressure sterilized ultra-pure water (used in *in vivo* experiment).

2.3 Models of diabetes and circadian rhythm

After adaptive feeding for several days, type-1 diabetes was generated in rats by intraperitoneally injecting animals with streptozotocin (STZ, Sigma, 65 mg/kg) dissolved in citrate buffer, as described previously [32–34]. Rats in the non-diabetic group were injected with the same amount of citrate buffer. 72 hours after STZ administration, blood was drawn from the tail vein of each rat once to measure fasting blood glucose (FBG). Rats exhibiting hyperglycemia (blood glucose levels higher than 16.7 mmol/L) were considered to have diabetes and continuously fed for at least 8 weeks. FBG and body weight were monitored weekly.

All animals were synchronized to a fixed 12 h light/12 h dark schedule (L/D cycle) — ZT0 (Zeitgeber Time) was set at 7:00 AM, and ZT12 at 7:00 PM — and placed in their home cages, with lighting set at 250 to 300 lux for each box. Their individual running periods and spells of activity onset were free of restriction and recorded daily.

2.4 Experimental protocols in vivo

At the end of the scheduled course, rats were tranquilized, and their apical blood was collected in anticoagulation tubes. Heart tissues were rapidly excised and washed with cold PBS and 0.9% Nacl. These heart tissues and blood samples were collected at ZT5, ZT11, ZT17, and ZT23 (n = 4/time point/group). Also, randomly chosen diabtic rats were treated with or without PF-670462 (30 mg/kg, i.p., n = 5/group) once at ZT11 and sacrificed at ZT23. Zeitgeber Time and dosage were applied as per previous dose-response rates [21,29,31], and all collected samples were stored at –80 °C for subsequent experiments. The general experimental design is shown in Fig. 1A.

2.5 Cardiac function

Cardiac function was monitored using an animal ultrasound cardiogram (UCG) to measure parameters, including IVSs, left ventricular EF%, and FS%. Two-dimensional and M-mode echocardiographic measurements were analyzed with a GE vivid 7 E95 high resolution *in vivo*-imaging system (VisualSonics, Toronto, ON, Canada).

2.6 RNA isolation and RT-PCR

Rat heart tissues were homogenized in TriReagent (Sigma) using a Liquid nitrogen grinding instrument (Mo Bio Laboratories Inc, Carlsbad, CA), and total RNA was isolated according to the manufacturer's instructions and reverse transcribed. SYBR Green qPCR was then applied to the reverse transcription product in real-time quantitative RT-PCR (Applied Biosystems 7500 Real-Time PCR System). The expression of genes within each sample was normalized against β-actin and communicated relative to a calibrator group using the formula $2^{-(\Delta\Delta Ct)}$. The following primer pairs were used for PCR analyses: for PER2, forward primer 5′-CCCAGCAAGTGATCGAGGACTA-3′, reverse primer 5′-TTGACACGCTTGGACTTC AGTT-3′; for β-actin as a housekeeping gene, forward primer 5′-TGCTATGTTGCC CTAGACTTCG-3′, reverse primer 5′-GTTGGCATAGAGGTCTTTA CGG -3′.

2.7 Blood biochemical testing

Blood glucose was determined using a portative glucometer, MediSense Optium Xceed (Abbott Diagnostics Ltd, Maidenhead, UK). The biochemical marker of myocardial injury, LDH, was assayed using an automatic biochemical analyzer (SIEMENS, ADVIA 2400, Germany).

2.8 TUNEL staining

Myocardial injury was quantified using a TdT-mediated dUTP nick-end labeling (TUNEL) technique in *in situ* slices utilizing a One Step TUNEL Apoptosis Assay

Kit (Beyotime, Jiangsu, China) according to the manufacturer's instructions. The nuclei were counterstained with a DAPI staining solution (Service, Wuhan, China) for 10 min at room temperature, and TUNEL signals were observed with fluorescence microscopy (Olympus, Japan). Finally, at least ten visual fields were randomly selected per slice, and their apoptosis index (AI) was presented as the ratio of TUNEL-positive cells to total cells quantified using ImageJ software (National Institutes of Health [NIH], Bethesda, MD, USA).

2.9 Cell culture and transfection

H9C2 cell lines were obtained from the Cell Bank of the Chinese Academy of Sciences (Shanghai, China) and routinely cultured in complete DMEM media containing 5 mM glucose and L-glutamine (Hyclone, USA) supplemented with 10% fetal bovine serum (Gibco Laboratories, USA) and 1% antibiotics (Gibco Laboratories, USA). The cells were cultured at 37 °C in a humidified atmosphere with 5% CO_2. Upon cells in the six-well plates reaching 75–85% confluence, they were incubated with serum-free DMEM containing 0.1% BSA for 12 h and then exposed to different treatments for 24 h: the various treatment groups included a low-glucose group (5.5 mM glucose, LG group), a high-glucose group (30 mM glucose, HG group), and a high-glucose + PF-670462 group (HG + PF group); PF-670462 was dissolved in DMSO and used at concentrations of 0.5, 1, 5, or 10 μM simultaneously with high glucose. Post-treatment, cells and cultured media were collected and stored separately for assessment.

For cell transfection, single-gene si-RNA kits (RIBOBIO, Guangzhou, China) were mixed with Lipofectamine 2000 (GLPBIO, USA) in Opti-MEM (Gibco, USA) and transfected into H9c2 cells according to the manufacturer's instructions. Each experiment was performed at least three times.

2.10 CCK-8 and LDH

Cell viability was determined using a CCK-8 Assay Kit (Jiancheng, Nanjing, China). Briefly, H9c2 cells were cultured and treated in 96-well plates, after which 10 μL of the CCK-8 reagent was added to each well, and the mixture was incubated for about 1 h in darkness to detect cell viability.

LDH in cultured media was measured using a colorimetric assay kit (Jiancheng, Nanjing, China) according to the manufacturer's instructions. Absorbance was spotted with the Perkin Elmer Microplate reader (EnSight PerkinElmer Victor 1420, USA).

2.11 Calcein-AM/PI

To observe live and dead cells in the culture dish concurrently, the Calcein-AM/PI assay (DOJINDO, Japan) was employed according to the manufacturer's instructions. In brief, H9c2 cells were loaded with calcein-AM and PI reagents at 37 °C for 15 min, and the fluorescence signal for Calcein-AM was detected at 490 nm excitation and 515 nm emission and that for PI at 530 nm excitation and 580 nm emission. The results were presented as the ratio of live to dead cells, as determined using Flow cytometry (BECKMAN COULTER, USA), and read with the Perkin Elmer Microplate reader (EnSight PerkinElmer Victor 1420, USA).

2.12 Western blotting

Cardiac or cell protein per group was extracted and separated on a 10% Tris·HCl Ready Gel (Bio-Rad) and transferred to a PVDF membrane, where it was blocked with 5% Skimmed milk powder in TBS-T (TBS plus 0.1% Tween 20). For the *in vivo* experiment, the protein extract was next incubated with antibodies against PER2 (1:1000, BD, 611138), phosphorylated PER2 (1:500, LSBio, LS-C357202), CK1ε (1:1000, CST, 12448S), or GAPDH (1:1000, CST, 5174S) overnight at 4 °C. Incubations for the *in vitro* experiment were carried out with antibodies against PER2 (1:1000, BD, 611138), phosphorylated PER2 (1:500, Abmart, TA4301S), CK1ε (1:1000, Proteintect, 11230-1-AP) or GAPDH (1:1000, Proteintect, 60004-1-Ig) overnight at 4 °C. The goat anti-rabbit IgG (H+L) (CST, USA, #5151P) or anti-mouse IgG (H+L) (CST, USA, #5257P) secondary antibody was added, as described previously [32–34]. Protein bands were detected with an Odyssey color infrared laser scan-imaging instrument (Li-Cor, USA) and analyzed using Image J software. GAPDH was used as a normalized control. Data were recorded as relative density ratios.

2.13 Histomorphology and immunofluorescence

Cardiac tissue samples from the *in vivo* experiment were fixed with 4% paraformaldehyde and paraffin and sliced into sections. For myocardial histomorphology observation, these sections were counterstained with Hematoxylin and Evans Blue (HE). Some sections per group were subjected to immunofluorescence (IF) with an anti-PER2 antibody (1:50, BD, 611138) to examine PER2's distribution in the heart.

In the H9c2 cell experiment, sterile coverslips were plated in 6-well plates, and 0.5~1 $\times$ 10^5 H9c2 cells were seeded per well and cultured. After culture to about 80% confluence, cells were washed with pre-cold PBS 3 times and fixed with 4% paraformaldehyde to create sections, which were counterstained with HE, as presented above, to observe cellular morphology and measure its parameter. Some slices were also subjected to IF with a PER2 antibody (1:100, Abclonal, A12694) and a CK1ε antibody (1:100, Abcam, Ab115293) to examine PER2's localization. Sections were photographed using a digital microscope (BX63, Olympus, Japan).

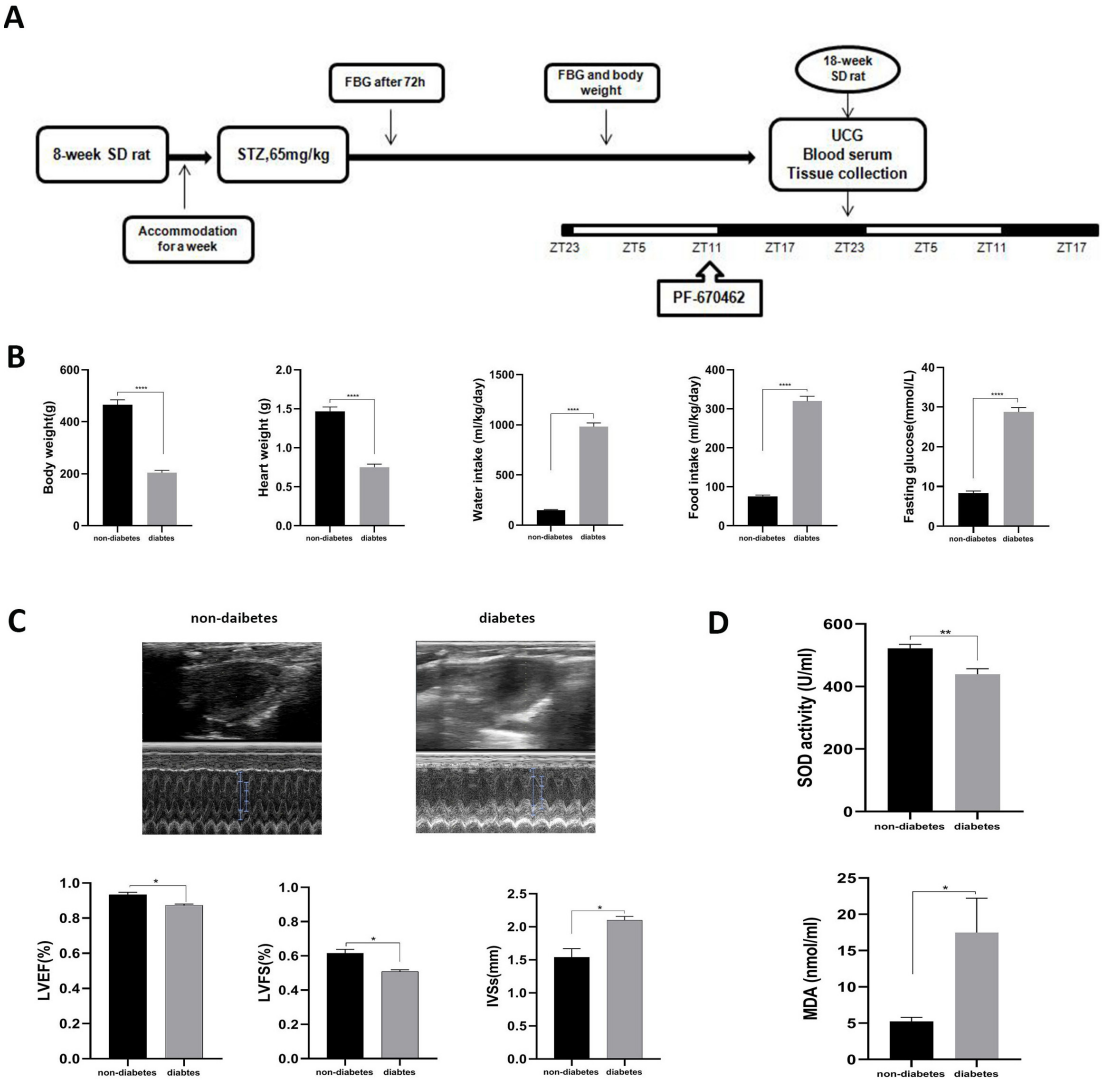

Fig. 1. General characteristics and the myocardial injury in STZ-induced diabetic rats. (A) Showed the general experimental design. (B) Showed the animals' genecral characteristics. (C) Showed the cardiac function measured by ultrasound cardiogram (UCG). (D) Showed the indicators of oxidation stress injury. Data was expressed as the Mean ± SEM, $*p < 0.05$, $**p < 0.01$ and $****p < 0.0001$ vs N Group analyzed by *Student's t-test*.

2.14 Statistical analysis

All data are expressed as the Mean ± SEM. A two-way ANOVA (time of day × groups) and *Fisher's LSD* test, in that order, were performed for rhythmic profiles. The Cosinor analysis software 3.1 was used to calculate the beat period, amplitude, and *p*-value [35–37]. Statistical analysis was conducted with the GraphPad Prism version 8.3.0 (GraphPad Software, USA). One-way ANOVA and *Fisher's LSD* test, in that order, were applied for multiple comparisons, and the *Student's t-test* was utilized for comparisons between two groups. p values < 0.05 were considered to be statistically significant. Correlations were assessed with Pearson's correlation coefficient (PCC) and Manders' colocalization coefficients (MCC), and their fluorescent scatter plots were automatically calculated and generated with Image J software 1.8.0.172 (National Institutes of Health [NIH], Bethesda, MD, USA)/Colo 2. A correlation coefficient of $|R| > 0.8$ indicated a high association between variables.

3. Results

3.1 STZ-induced diabetes altered the general features of rats and caused myocardial injury

Compared to age-matched non-diabetic rats (N Group), diabetic rats (DM Group) exhibited obvious diabetic symptoms, such as high glucose, polydipsia, polyphagia, polyuria, weight loss, sour litter, and more. General characteristics, including body weight, heart weight, water intake, food intake, and FBG, were significantly altered in STZ-induced diabetic rats compared to their control counterparts (Fig. 1B). For cardiac function, diabetic rats displayed lower LVEF and LVFS and higher IVSs than

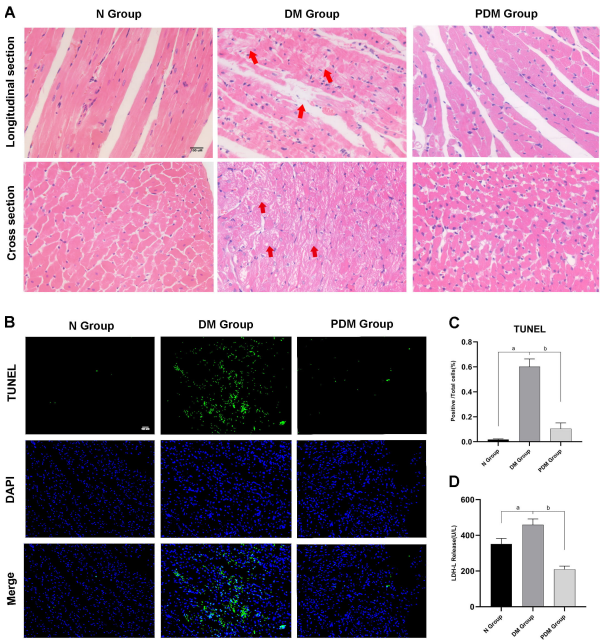

Fig. 2. Observation and quantification of cardiac injuries. (A) HE pictures showing myocardial histomorphological changes of different groups from its longitudinal and cross section (magnification $\times$400). N group: regular myocardial fibers and cardiomyocytes; DM group: mass disordered myocardial fibers, irregular and even dissolved vacuolated myocardiocytes with interstitial edema; PDM group: a small amount of vacuoles and lysis in the cytoplasm. (B) Observation of the green fluorescence to detect the level of cardiac apoptosis (magnification $\times$200). Each group had at least 5 cardiac sections, and each slice was randomly observed and photographed at least 10 fields. TUNEL: green; DAPI: Blue; Scale bar = 100 uM. (C) and (D) Quantification of the extent of cardiac injury respectively by apoptosis positive rate % and LDH reslease. Data was expressed as the Mean $\pm$ SEM, $^{a}p < 0.05$ vs N Group, $^{b}p < 0.05$ vs PDM Group analyzed by one-way ANOVA followed by *Fisher's LSD test*.

non-diabetic rats (Fig. 1C). Furthermore, biochemical measurements registered substantially elevated MDA levels and a drop in SOD activity in the DM Group relative to the N Group (Fig. 1D). Myocardial morphology assessments (HE) established a series of myocardial damages, including disordered myocardial fibers and irregular and even dissolved vacuolated myocardiocytes with interstitial edema, in the DM Group compared to the N Group (Fig. 2A). Simultaneously, the apoptosis rate quantifying myocardial injury was higher in the DM Group than in the N Group (Fig. 2B,C).

3.2 STZ-induced diabetes altered the oscillation of PER2 and CK1ε

This study showed that diabetes markedly influenced the expression of PER2 and CK1ε. PER2 mRNA levels increased at ZT5 and ZT23 and decreased at ZT11 and ZT17 in the DM Group compared to the N Group (Fig. 3A). Moreover, at the protein level, PER2 expression oscillated both in the N Group and DM Group (Fig. 3B). PER2 exhibited a phase delay and a lower amplitude in the DM Group relative to the N Group (Table 1). CK1ε protein levels oscillated significantly in the N and DM Groups (Fig. 3C). Compared to the N Group, the amplitude of CK1ε expression rose in the DM Group but with no phase shift (Table 1).

Table 1. Cosinor analysis of PER2 and CK1ε protein expression in the heart.

Protein	Groups	Amplitude	Phase (h)	*p*-value
PER2	N Group	17.0518	23.7	0.000458
	DM Group	16.2469	24.1	0.005074
CK1ε	N Group	17.1454	23.8	0.000029
	DM Group	17.184	23.8	0.000024

When quantification of PER2 and CK1ε expression revealed a significant rhythm ($^{*}p < 0.05$ analyzed by two-way ANOVA), datas were fitted with a Cosinor analysis. For the best period, the cosinor parameters (Period, Amplitude, *p*-Value) are displayed. The cosine fit was considered to be statistically significant when F was greater than $F_{0.05}$ ($^{*}F > F_{0.05}$).

3.3 PF-670462 inhibited the expression of CK1ε and phosphorylated PER2 and attenuated myocardial injury in diabetic rats

We measured the protein levels of CK1ε and phosphorylated PER2 at ZT23 and found that the expression of CK1ε and phosphorylated PER2 in the DM Group increased compared to the N Group. Inhibiting CK1ε with its inhibitor (PF-670462) diminished the PDM Group's phosphorylated PER2 levels relative to the DM Group (Fig. 4A and B). Additionally, IF analyses revealed that PER2 was distributed in both the nucleus and cytoplasm of rats in different groups (Fig. 4C).

After treating diabetic rats with PF-670462 (PDM Group), we observed that their hair and cages became slightly dry and clean, and their activity levels improved spontaneously compared to diabetic rats (DM Group). While diabetes-caused myocardial structural damage remained notable in the PDM group, there were no longer dense masses of vacuolated cardiomyocytes and dissolved myocardial fibers (Fig. 2A). Also, the apoptosis rate and the biomarker of myocardial injury, LDH, dwindled in the PDM Group relative to the DM Group (Fig. 2B,C,D).

3.4 High glucose caused cell injury and augmented PER2 and CK1ε signaling in H9c2

Consistent with our previous experiments [32–34], HG prompted a decrease in cell viability and an increase in LDH release and the dead/live rate compared to the LG

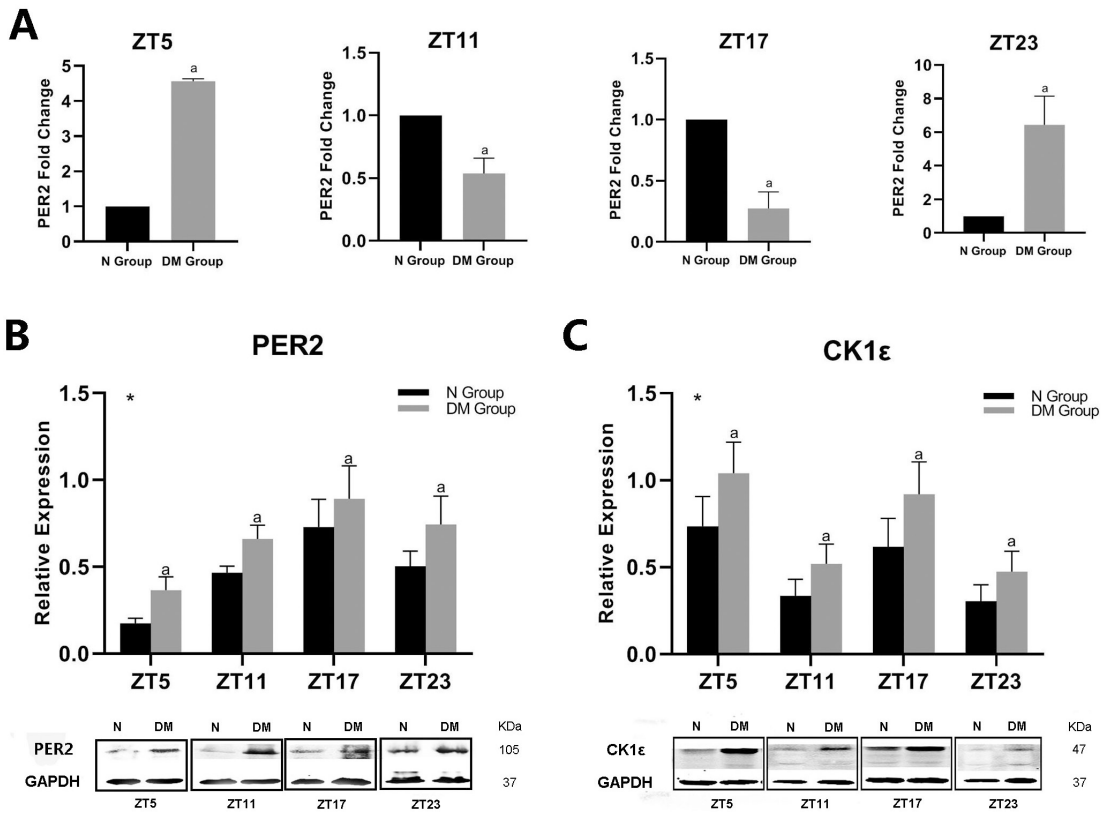

Fig. 3. Effect of diabetes on PER2 and CK1ε signaling. (A) showed the effect of diabetes on PER2 in mRNA level respectively at ZT5, ZT11, ZT17 and ZT23. Data was expressed as the Mean ± SEM, $^{a}p < 0.05$ vs N Group analyzed by Student's *t*-test. (B) and (C) respectively showed the effect of diabetes on PER2 and CK1ε in Protein level. Data was expressed as the Mean ± SEM, n = 4/time point/group, $*p < 0.05$ indicated its rhmthy, $^{a}p < 0.05$ vs N Group both analyzed by two-way ANOVA followed by *Fisher's LSD* test.

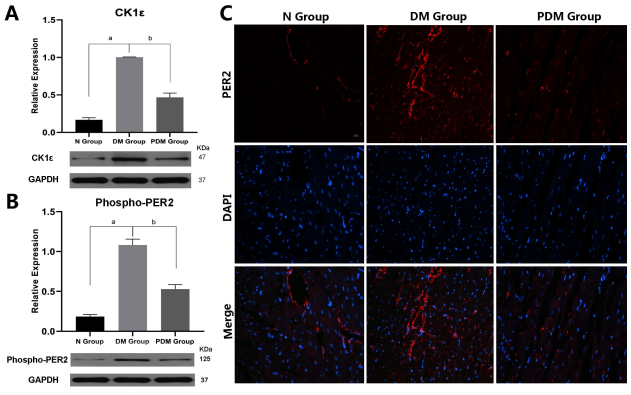

Fig. 4. PF-670462 remedied the expression of CK1ε and phosphorylated PER2 during diabetes. (A)and (B) Quantifying relative expression of CK1ε and phosphorylated PER2 by western blotting. Data was expressed as the Mean ± SEM, $^{a}p < 0.05$ vs N Group, $^{b}p < 0.05$ vs PDM Group analyzed by one-way ANOVA followed by *Fisher's LSD test*. (C) Representative fluorescent micrographs showing PER2's distribution in cardiac sections for different groups (Positive PER2, red; DAPI for nucleus, blue; magnification ×200).

group (Figs. 5A,B, 6C,D). Evaluations of H9c2 cells with HE highlighted a more hypertrophic cell shape and lower cell density in the HG Group than in the LG group (Fig. 6A and B). Additionally, CK1ε, phosphorylated PER2, and PER2 protein expressions were amplified in the HG group relative to the LG group (Fig. 5C).

As shown in Fig. 6E, CK1ε and PER2 were expressed both in the nucleus and cytoplasm. We also found that high glucose heightened phosphorylated PER2 levels and the nuclear-cytoplasmic ratio of PER2 (Figs. 5C, 6E,G). Meanwhile, the analysis of the relationship between CK1ε and PER2 using IF established that CK1ε and PER2 correlated highly, with Pearson's R ranging from 0.71 to 0.83 and Manders' M value ranging from 0.997 to 1 (Fig. 6F).

3.5 Inhibiting CK1ε-regulated PER2 alleviated HG-induced cell injury in H9c2

Exposing H9c2 cells to high glucose and treating them with 0.5 μM, 1 μM, 5 μM, or 10 μM of PF-670462 yielded different results: 0.5 μM and 1 μM of PF-670462 considerably increased cell viability and decreased LDH release (Fig. 5A and B), while concentrations of PF-670462 exceeding 1 μM failed to ignite any drastic reduction in LDH release or intensify H9c2 cell activity. Nevertheless, cell

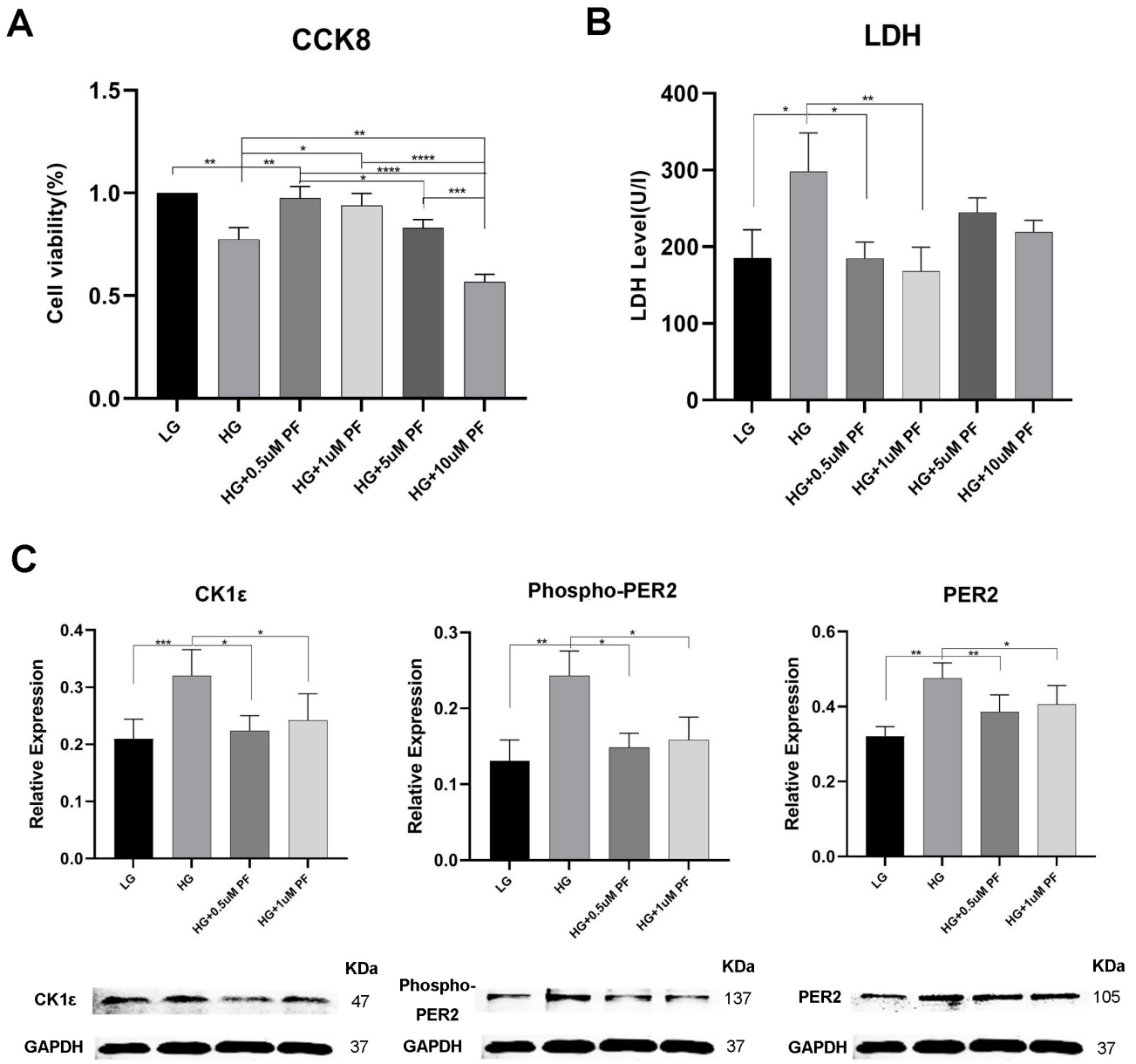

Fig. 5. The effect of PF-670462 on PER2 and CK1ε in high-glucose condition. (A) and (B) Quantification of cell viability and LDH level. (C) Quantification of protein expression of CK1ε, phosphorylated PER2 and PER2 by western blotting in different groups. Data was expressed as the Mean $\pm$ SEM, and repeated-measures analysis was at least three times for each group. *$p < 0.05$, **$p < 0.01$, ***$p < 0.001$ and ****$p < 0.0001$ analyzed by one-way ANOVA followed by *Fisher's LSD test*.

shape was regular, cell density increased, and cell mean area was smaller in the HG+PF group compared to the HG group (Fig. 6A and B). Also, the ratio of dead/live cells declined (Fig. 6C and D).

H9c2 cell treatment with PF-670462 in high glucose conditions saw a fall in the expression of CK1ε, phosphorylated PER2, and PER2 in the HG + PG group (Fig. 5C) and a reduction in the nucleus-cytoplasm ratio of PER2 in the HG + PF group compared to the HG group (Figs. 5C, 6E,G).

As shown in Fig. 7A and B, knocking down PER2 in the presence of high glucose resulted in improved cell viability relative to the controls. PF-670462's attempt to down-regulate PER2 and improve cell viability in high glucose conditions beyond the rates achieved by PER2 knockdown was comparable to that of HG+si-PER2 (Fig. 7A and B).

4. Discussion

This investigation contributes to growing evidence that molecular clockwork is compromised during diabetes. It revealed that diabetes resets PER2's oscillation in association with activated CK1ε signaling to phosphorylate PER2 at Ser662 and translocate PER2 into the nucleus. We also confirmed that inhibiting CK1ε-regulated PER2 attenuates myocardial injuries in high glucose conditions.

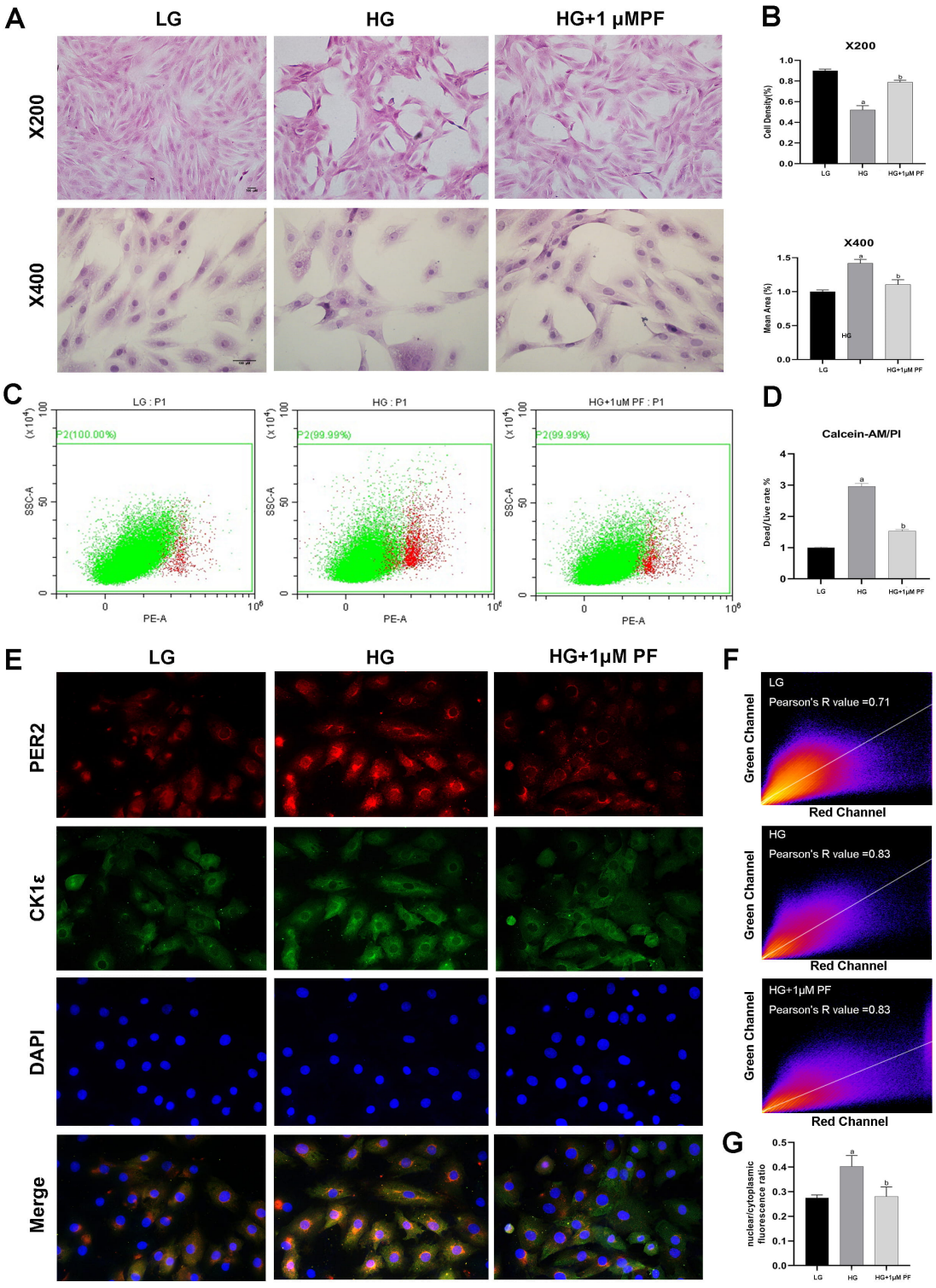

Fig. 6. Assessment of cell injuries and distributions of PER2 in H9c2. (A) and (B) Representing respectively observation and quantification of histomorphological structure of different groups in H9c2 (magnification ×200 and ×400). (C) and (D) Quantification of the rate of dead/live cells by a Flow cytometry. (E) Observation the distribution of PER2 and CK1ε by immunofluoresce in H9c2. Positive PER2: red, CK1ε: green, DAPI for nucleus:blue; Scale bar = 100 uM, magnification ×400. (F) Analysis the correlation of PER2 and CK1ε by Pearson's correlation coefficient (PCC) and Manders' Colocalization Coefficients (MCC) by Image J/Colo 2. (G) Quantification the ratio of nuclear to cytoplasm of PER2 via immunofluoresce. Data was expressed as the Mean ± SEM, and repeated-measures analysis was at least three times for each group. $^{a}p < 0.05$ vs N Group, $^{b}p < 0.05$ vs PDM Group analyzed by one-way ANOVA followed by *Fisher's LSD test.*

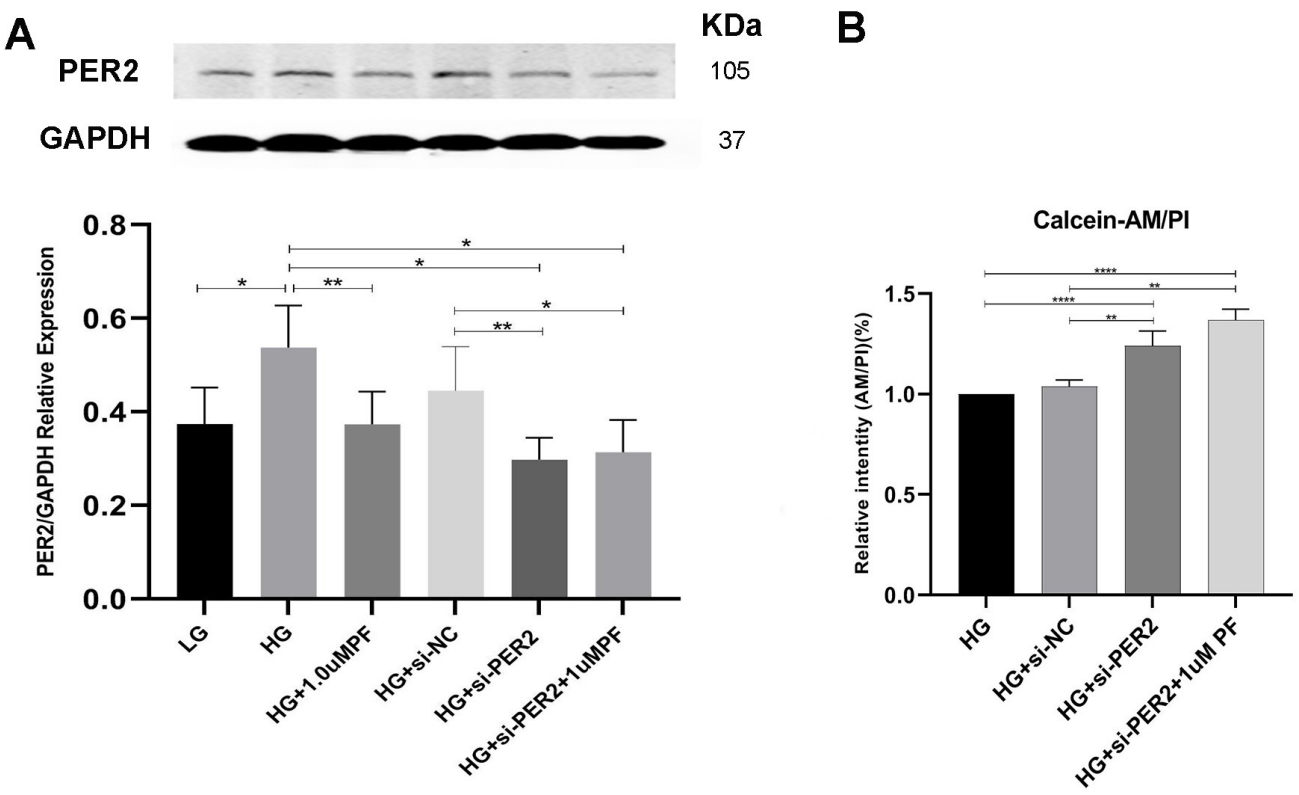

Fig. 7. Pharmacological and genetic targeting of PER2 in high-glucose condition. (A) Quantification of protein expression of PER2 treated with PF-670462 or siRNA in high-glucose condition. (B) Relative intentity of Calcein-AM/PI detected by fluorescent Microplate reader. Data was expressed as the Mean ± SEM, $*p < 0.05$, $**p < 0.01$ and $****p < 0.0001$ analyzed by one-way ANOVA followed by *Fisher's LSD test*.

Diabetes mellitus is now one of the most prevalent disorders, and it could lead to devastating myocardial injuries on the cardiac structure and function [1–3]. Cardiovascular disease (CVD) is the leading cause of death in type-1 and type-2 diabetes, and, while >80% of the population suffers from type-2 diabetes, type-1 diabetes results in more emergencies and is usually selected as a model for studying potential diabetic mechanisms. At present, the STZ-induced diabetes model and the high glucose in H9c2 cells model are universally adopted for the examination of the potential molecular mechanisms of diabetes [38,39]. These two models were also applied in our study and verified that diabetes-associated hyperglycemia triggered adverse myocardial injuries (Figs. 1C, 2A,B,C, 5A,B, 6A,B,C,D). The pathophysiology of a diabetic myocardial injury is complex and multifactorial, and uncovering its potential molecular *modus operandi* could benefit diabetic patients.

Although some studies have reported the impact of diabetes on PER2 [40–43], a clear understanding of the extent of its influence and its potential mechanism must still be explored. Consistent with what other studies have demonstrated [42–44], we found that diabetes altered PER2 expression at the mRNA level at different time points (Fig. 3A). Investigations have shown that the PER2 protein acts as a remarkable functional regulator through its cyclic accumulation and degradation in mammals [14–16]. Based on this, we examined the oscillation of the PER protein and established that diabetes changed PER's stability, with its phase delayed and amplitude decreased (Fig. 3B). The stability of PER2 depends on its phosphorylation status, and the rivalry between two unique competing sites on the PER2 protein is the key step in the PER2 circadian phosphoswitch that determines its period.

There is proof that CK1δ/ε primes the PER2 circadian phosphoswitch mainly at Ser662, which slows the rate of PER2 protein degradation, guides its nuclear entry, and regulates transcriptional repressor activity to determine PER2 period length [12,24,45]. Different forms of CK1 may have differing abilities to phosphorylate PER2 to control its period; however, that change in a single amino acid in CK1ε (CK1ε tau) in hamsters and mice shortens PER's period and loses temperature compensation is confirmation that CK1ε regulates PER2 [27,28]. Thus, in this study, we also assessed the effect of diabetes on CK1ε signaling. According to the results obtained, CK1ε showed an oscillation in the heart, matching the rhythmic oscillation reported previously in the suprachiasmatic nucleus [26,28], and diabetes increased the coincidence of CK1ε amplification with a PER2 phase delay (Fig. 3C). We hypothesized that CK1ε signaling could be a breakthrough in uncovering the con-

nection between diabetes and PER2 and chose a single time point to explore this potential further. The findings indicated that subjecting both the *in vivo* and H9c2 cell experiments to high-glucose prompted an upregulation of CK1ε and phosphorylated PER2 at Ser662 (Fig. 4A, 4B and 5C). Inhibiting activated CK1ε signaling with PF-670462 culminated in reduced phosphorylation at Ser662 and nuclear translocation of PER2 (Figs. 4A,B, 5C, 6E and G), supporting the hypothesis that CK1ε signaling plays a regulatory role in delaying the PER2 phase during diabetes. Although the antibody against phospho-PER2 used in the *in vivo* and H9c2 cell experiments were purchased from two differrent company and its molecular mass have slight discrepancy (**Supplementary figures**), both of this two antibodies detect endogenous levels of PER2 only when phosphorylated at Ser662.

Targeting CK1ε-regulated PER2 could benefit diabetes, as others have reported the role of the clock gene, Bmal1, in high glucose-induced cardiomyocyte injuries too [4,44]. In our study, knocking down PER2 in H9c2 using si-RNA in H9c2 in the presence of high-glucose lessened the incidence of high-glucose-instigated injuries (Fig. 7A and B), substantiating the hypothesis that targeting PER2 benefits myocardial injury healing in high-glucose conditions. Attention is increasingly being paid to the pharmacological manipulation of the molecular clock to alleviate injuries under different pathological circumstances [46–48]. Remarkably, we also found in our inquiry that PF-670462, to some extent, ameliorated high-glucose-generated myocardial injury, besides targeting CK1ε-regulated PER2 (Figs. 5A,B,C, 6A,B,C,D, 7A,B). Both genetic and pharmacological engineering methods have contributed to identifying the role of PER2 in high glucose-caused injuries.

As demonstrated in previous studies, PF-670462 slows down PER protein turnover and lengthens the circadian period in normal animals [21,29–31]. Currently, the number of investigations reporting that the impact of PF-670462 relies on the status of PER2 being influenced by metabolic and environmental stimuli are mounting [12,24,46–48]. In our research, PF-670462 exhibited no influence on PER2 expression and cell injury when PER2 was knocked down in the presence of high glucose (Fig. 7A and B), suggesting that PF-670462 aids high-glucose-engendered injuries only when the PER2 protein is upregulated, consistent with a report that PF-670462 inhibits IgE-mediated allergic reactions only when PER2 is increased [48].

Despite its promising revelations, our study had several limitations. Due to financial constraints, we have not used PER2$^{-/-}$ mice to further validate the above regulatory mechanism. Additionally, in our study, administering PF-670462 once had no marked effect on diabetic hyperglycemia, which contradicts the finding that pharmacologically targeting the circadian clock long-term via CK1δ/ε improves glucose homeostasis [8]. Whether adjusting the dosage and mode of PF-670462 application might bring about more significant benefits to diabetes treatment needs to be scrutinized in the future. Also, we hope that our investigation will provide important new insights into diabetic myocardial injuries.

5. Conclusions

In summary, this work first provides additional evidence that diabetes compromises PER2 in association with activated CK1ε signaling. Furthermore, it shows that targeting CK1ε-regulated PER2 alleviates myocardial injuries in high-glucose conditions. This mechanism provides a promising therapeutic strategy for diabetic myocardial injury treatment despite requiring further examination.

Author contributions

ZYX, SL and QH designed the research study. QH and MJ performed the research. QH and ZQ analyzed the data and wrote the manuscript. ZYX, SL, BZ, MJ, ZQ, and QH contributed to editorial changes in the manuscript. All authors read and approved the final manuscript.

Ethics approval and consent to participate

All institutional and national guidelines for the care and use of laboratory animals were followed. The protocols used on all the animals have been reviewed and approved by the Institutional Animal Care and Use Committee (IACUC) of Renmin Hospital of Wuhan University (#20180214).

Acknowledgment

The authors would like to thank the Central Laboratory of Remin Hospital of Wuhan University for the expert technical assistance.

Funding

This study was supported by grants from National Natural Science Foundation of China [grant number: 81671891] and [grant number: 81901947]. The organization had no role in the design of the study, the collection, analysis, and interpretation of data and writing the manuscript.

Conflict of interest

The authors declare no conflict of interest.

Supplementary material

Supplementary material associated with this article can be found, in the online version, at https://www.imrpress.com/journal/FBL/27/2/10.31083/j.fbl2702058.

References

[1] Amiel SA, Aschner P, Childs B, Cryer PE, de Galan BE, Frier BM, *et al*. Hypoglycaemia, cardiovascular disease, and mortal-

ity in diabetes: epidemiology, pathogenesis, and management. The Lancet Diabetes & Endocrinology. 2019; 7: 385–396.
[2] International Diabetes Federation. IDF Diabetes Atlas. 9th edn. International Diabetes Federation. 2019.
[3] Bugger H, Abel ED. Molecular mechanisms of diabetic cardiomyopathy. Diabetologia. 2014; 57: 660–671.
[4] Hou T, Su W, Guo Z, Gong MC. A Novel Diabetic Mouse Model for Real-Time Monitoring of Clock Gene Oscillation and Blood Pressure Circadian Rhythm. Journal of Biological Rhythms. 2019; 34: 51–68.
[5] Alex A, Li A, Zeng X, Tate RE, McKee ML, Capen DE, *et al*. A Circadian Clock Gene, Cry, Affects Heart Morphogenesis and Function in Drosophila as Revealed by Optical Coherence Microscopy. PLoS ONE. 2015; 10: e0137236.
[6] Young ME, Brewer RA, Peliciari-Garcia RA, Collins HE, He L, Birky TL, *et al*. Cardiomyocyte-Specific BMAL1 Plays Critical Roles in Metabolism, Signaling, and Maintenance of Contractile Function of the Heart. Journal of Biological Rhythms. 2014; 29: 257–276.
[7] Virag JAI, Dries JL, Easton PR, Friesland AM, DeAntonio JH, Chintalgattu V, *et al*. Attenuation of myocardial injury in mice with functional deletion of the circadian rhythm gene mPer2. American Journal of Physiology-Heart and Circulatory Physiology. 2010; 298: H1088–H1095.
[8] Cunningham PS, Ahern SA, Smith LC, da Silva Santos CS, Wager TT, Bechtold DA. Targeting of the circadian clock via CK1δ/ε to improve glucose homeostasis in obesity. Scientific Reports. 2016; 6: 29983.
[9] Qiao L, Guo B, Zhang H, Yang R, Chang L, Wang Y, *et al*. The clock gene, brain and muscle Arnt-like 1, regulates autophagy in high glucose-induced cardiomyocyte injury. Oncotarget. 2017; 8: 80612–80624.
[10] Dyar KA, Ciciliot S, Wright LE, Biensø RS, Tagliazucchi GM, Patel VR, *et al*. Muscle insulin sensitivity and glucose metabolism are controlled by the intrinsic muscle clock. Molecular Metabolism. 2013; 3: 29–41.
[11] Hennig S, Strauss HM, Vanselow K, Yildiz O, Schulze S, Arens J, *et al*. Structural and functional analyses of PAS domain interactions of the clock proteins Drosophila PERIOD and mouse PERIOD2. PLOS Biology. 2009; 7: e94.
[12] Zhou M, Kim JK, Eng GWL, Forger DB, Virshup DM. A Period2 Phosphoswitch Regulates and Temperature Compensates Circadian Period. Molecular Cell. 2015; 60: 77–88.
[13] Kucera N, Schmalen I, Hennig S, Öllinger R, Strauss HM, Grudziecki A, *et al*. Unwinding the differences of the mammalian PERIOD clock proteins from crystal structure to cellular function. Proceedings of the National Academy of Sciences of the United States of America. 2012; 109: 3311–3316.
[14] Yildiz O, Doi M, Yujnovsky I, Cardone L, Berndt A, Hennig S, *et al*. Crystal structure and interactions of the PAS repeat region of the Drosophila clock protein PERIOD. Molecular Cell. 2005; 17: 69–82.
[15] Chen R, Schirmer A, Lee Y, Lee H, Kumar V, Yoo S, *et al*. Rhythmic per abundance defines a critical nodal point for negative feedback within the circadian clock mechanism. Molecular Cell. 2009; 36: 417–430.
[16] Liu J, Zou X, Gotoh T, Brown AM, Jiang L, Wisdom EL, *et al*. Distinct control of PERIOD2 degradation and circadian rhythms by the oncoprotein and ubiquitin ligase MDM2. Science Signaling. 2018; 11: eaau0715.
[17] Dibner C, Schibler U, Albrecht U. The Mammalian Circadian Timing System: Organization and Coordination of Central and Peripheral Clocks. Annual Review of Physiology. 2010; 72: 517–549.
[18] Mavroudis PD, DuBois DC, Almon RR, Jusko WJ. Daily variation of gene expression in diverse rat tissues. PLoS ONE. 2018; 13: e0197258.
[19] Shi S, Ansari TS, McGuinness OP, Wasserman DH, Johnson CH. Circadian disruption leads to insulin resistance and obesity. Current Biology. 2013; 23: 372–381.
[20] Lemmer B, Oster H. The Role of Circadian Rhythms in the Hypertension of Diabetes Mellitus and the Metabolic Syndrome. Current Hypertension Reports. 2018; 20: 43.
[21] Meng Q, Maywood ES, Bechtold DA, Lu W, Li J, Gibbs JE, *et al*. Entrainment of disrupted circadian behavior through inhibition of casein kinase 1 (CK1) enzymes. Proceedings of the National Academy of Sciences of the United States of America. 2010; 107: 15240–15245.
[22] Gerbeth C, Schmidt O, Rao S, Harbauer A, Mikropoulou D, Opalińska M, *et al*. Glucose-Induced Regulation of Protein Import Receptor Tom22 by Cytosolic and Mitochondria-Bound Kinases. Cell Metabolism. 2013; 18: 578–587.
[23] Xu P, Fischer-Posovszky P, Bischof J, Radermacher P, Wabitsch M, Henne-Bruns D, *et al*. Gene expression levels of Casein kinase 1 (CK1) isoforms are correlated to adiponectin levels in adipose tissue of morbid obese patients and site-specific phosphorylation mediated by CK1 influences multimerization of adiponectin. Molecular and Cellular Endocrinology. 2015; 406: 87–101.
[24] Narasimamurthy R, Hunt SR, Lu Y, Fustin J, Okamura H, Partch CL, *et al*. CK1δ/ε protein kinase primes the per2 circadian phosphoswitch. Proceedings of the National Academy of Sciences. 2018; 115: 5986–5991.
[25] Agostino PV, Plano SA, Golombek DA. Circadian and pharmacological regulation of casein kinase i in the hamster suprachiasmatic nucleus. Journal of Genetics. 2008; 87: 467–471.
[26] Price JL, Fan J, Keightley A, Means JC. The role of casein kinase i in the Drosophila circadian clock. Methods in Enzymology. 2015; 551: 175–195.
[27] Meng QJ, Logunova L, Maywood ES, Gallego M, Lebiecki J, Brownet TM, *et al*. Setting clock speed in mammals: the CK1 epsilon tau mutation in mice accelerates circadian pacemakers by selectively destabilizing PERIOD proteins. Neuron. 2008; 58: 78–88.
[28] Maywood ES, Chesham JE, Smyllie NJ, Hastings MH. The Tau mutation of casein kinase 1ε sets the period of the mammalian pacemaker via regulation of Period1 or Period2 clock proteins. Journal of Biological Rhythms. 2014; 29: 110–118.
[29] Badura L, Swanson T, Adamowicz W, Adams J, Cianfrogna J, Fisher K, *et al*. An inhibitor of casein kinase i epsilon induces phase delays in circadian rhythms under free-running and entrained conditions. The Journal of Pharmacology and Experimental Therapeutics. 2007; 322: 730–738.
[30] Kim JK, Forger DB, Marconi M, Wood D, Doran A, Wager T, *et al*. Modeling and validating chronic pharmacological manipulation of circadian rhythms. CPT: Pharmacometrics & Systems Pharmacology. 2013; 2: e57.
[31] Kennaway DJ, Varcoe TJ, Voultsios A, Salkeld MD, Rattanatray L, Boden MJ. Acute inhibition of casein kinase 1δ/ε rapidly delays peripheral clock gene rhythms. Molecular and Cellular Biochemistry. 2015; 398: 195–206.
[32] Qiu Z, Ming H, Lei S, Zhou B, Zhao B, Yu Y, *et al*. Roles of HDAC3-orchestrated circadian clock gene oscillations in diabetic rats following myocardial ischaemia/reperfusion injury. Cell Death & Disease. 2021; 12: 43.
[33] Wu Y, Leng Y, Meng Q, Xue R, Zhao B, Zhan L, *et al*. Suppression of Excessive Histone Deacetylases Activity in Diabetic Hearts Attenuates Myocardial Ischemia/Reperfusion Injury via Mitochondria Apoptosis Pathway. Journal of Diabetes Research. 2017; 2017: 8208065.
[34] Qiu Z, Ming H, Zhang Y, Yu Y, Lei S, Xia ZY. The Protective Role of Bmal1-Regulated Autophagy Mediated by

HDAC3/SIRT1 Pathway in Myocardial Ischemia/Reperfusion Injury of Diabetic Rats. Cardiovascular Drugs and Therapy. 2021. (in press)
[35] Refinetti R, Earle G, Kenagy GJ. Exploring determinants of behavioral chronotype in a diurnal-rodent model of human physiology. Physiology & Behavior. 2019; 199: 146–153.
[36] Refinetti R. Western diet affects the murine circadian system possibly through the gastrointestinal microbiota. Biological Rhythm Research. 2019; 48: 287–296.
[37] Wassmer T, Refinetti R. Daily Activity and Nest Occupation Patterns of Fox Squirrels (Sciurus niger) throughout the Year. PLoS ONE. 2016; 11: e0151249.
[38] Li X, Ke X, Li Z, Li B. Vaspin prevents myocardial injury in rats model of diabetic cardiomyopathy by enhancing autophagy and inhibiting inflammation. Biochemical and Biophysical Research Communications. 2019; 514: 1–8.
[39] Huang L, Yuan P, Yu P, Kong Q, Xu Z, Yan X, *et al*. O-GlcNAc-modified SNAP29 inhibits autophagy-mediated degradation via the disturbed SNAP29-STX17-VAMP8 complex and exacerbates myocardial injury in type i diabetic rats. International Journal of Molecular Medicine. 2018; 42: 3278–3290.
[40] Eckel-Mahan KL, Patel VR, de Mateo S, Orozco-Solis R, Ceglia NJ, Sahar S, *et al*. Reprogramming of the circadian clock by nutritional challenge. Cell. 2013; 155: 1464–1478.
[41] Marcheva B, Ramsey KM, Buhr ED, Kobayashi Y, Su H, Ko CH, *et al*. Disruption of the clock components CLOCK and BMAL1 leads to hypoinsulinaemia and diabetes. Nature. 2010; 466: 627–631.
[42] Young ME, Wilson CR, Razeghi P, Guthrie PH, Taegtmeyer H. Alterations of the circadian clock in the heart by streptozotocin-induced diabetes. Journal of Molecular and Cellular Cardiology. 2002; 34: 223–231.
[43] Song F, Xue Y, Dong D, Liu J, Fu T, Xiao C, *et al*. Insulin Restores an Altered Corneal Epithelium Circadian Rhythm in Mice with Streptozotocin-induced Type 1 Diabetes. Scientific Reports. 2016; 6: 32871.
[44] Herichová I, Zeman M, Stebelová K, Ravingerová T. Effect of streptozotocin-induced diabetes on daily expression of per2 and dbp in the heart and liver and melatonin rhythm in the pineal gland of Wistar rat. Molecular and Cellular Biochemistry. 2005; 270: 223–229.
[45] Xu Y, Toh KL, Jones CR, Shin J, Fu Y, Ptácek LJ. Modeling of a human circadian mutation yields insights into clock regulation by per2. Cell. 2007; 128: 59–70.
[46] Janovska P, Verner J, Kohoutek J, Bryjova L, Gregorova M, Dzimkova M, *et al*. Casein kinase 1 is a therapeutic target in chronic lymphocytic leukemia. Blood. 2018; 131: 1206–1218.
[47] Keenan CR, Langenbach SY, Jativa F, Harris T, Li M, Chen Q, *et al*. Casein Kinase 1δ/ε Inhibitor, PF670462 Attenuates the Fibrogenic Effects of Transforming Growth Factor-β in Pulmonary Fibrosis. Frontiers in Pharmacology. 2018; 9: 738.
[48] Nakamura Y, Nakano N, Ishimaru K, Ando N, Katoh R, Suzuki-Inoue K, *et al*. Inhibition of IgE-mediated allergic reactions by pharmacologically targeting the circadian clock. Journal of Allergy and Clinical Immunology. 2016; 137: 1226–1235.